Electronic Supplementary Information

Facile synthesis of 3D few-layer MoS_2 coated TiO_2 nanosheet core-shell nanostructures for stable and high-performance lithium-ion batteries

Biao Chen,[a] Naiqin Zhao,[*a, b] Lichao Guo,[a] Fang He,[a] Chunsheng Shi,[a] Chunnian He,[a,b] Jiajun Li[a] and Enzuo Liu[*a, b]

[a] School of Materials Science and Engineering and Tianjin Key Laboratory of Composite and Functional Materials, Tianjin University, Tianjin 300072, P.R. China. E-mail: ezliu@tju.edu.cn, nqzhao@tju.edu.cn
[b] Collaborative Innovation Centre of Chemical Science and Engineering, Tianjin 300072, P.R. China

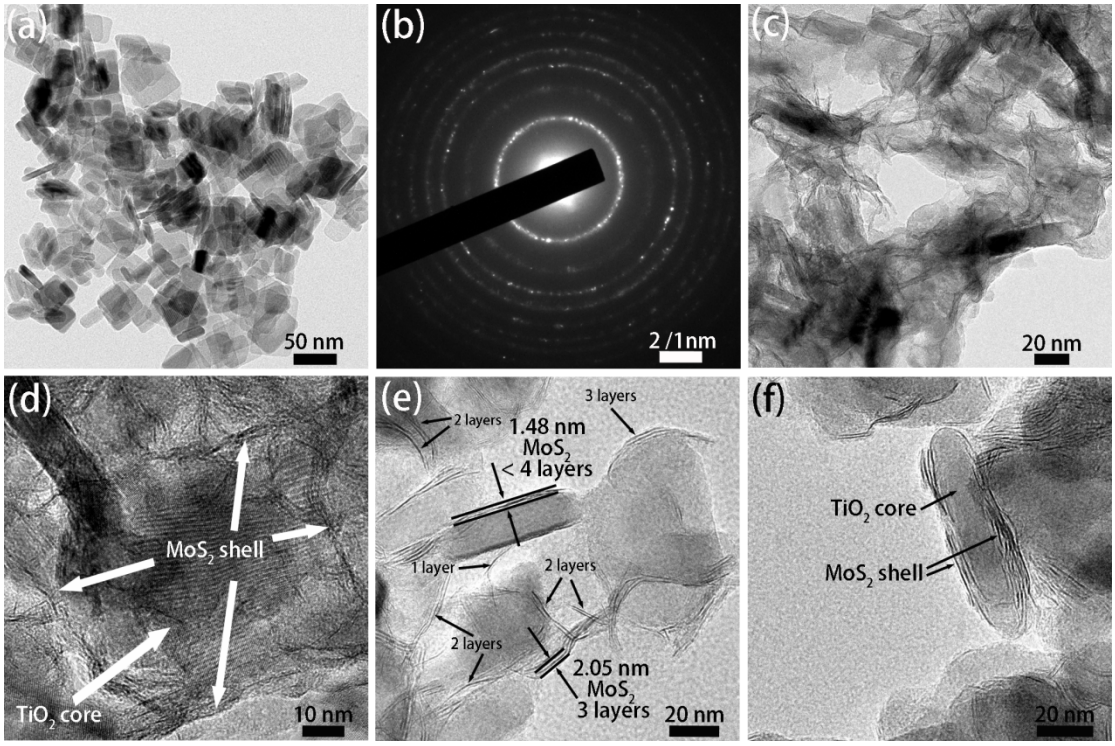

Fig. S1 (a) TEM image and (b) corresponding SAED pattern of F-TiO_2, (c, d) TEM images of 3D FL-MoS_2@TiO_2 before thermal-treated, (e, f) High-resolution TEM images of 3D FL-MoS_2@TiO_2.

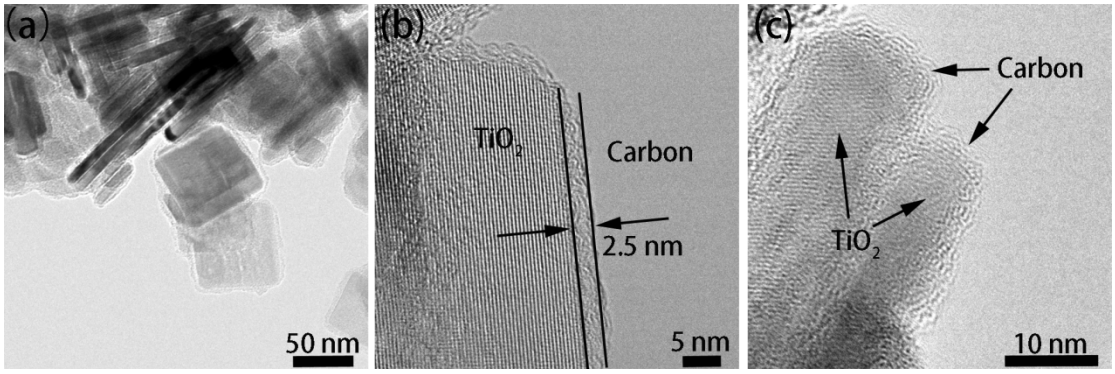

Fig. S2 (a-c) TEM images of hydrothermal products of the complex of F-TiO_2/glucose without Na_2MoO_4-CN_2H_4S.

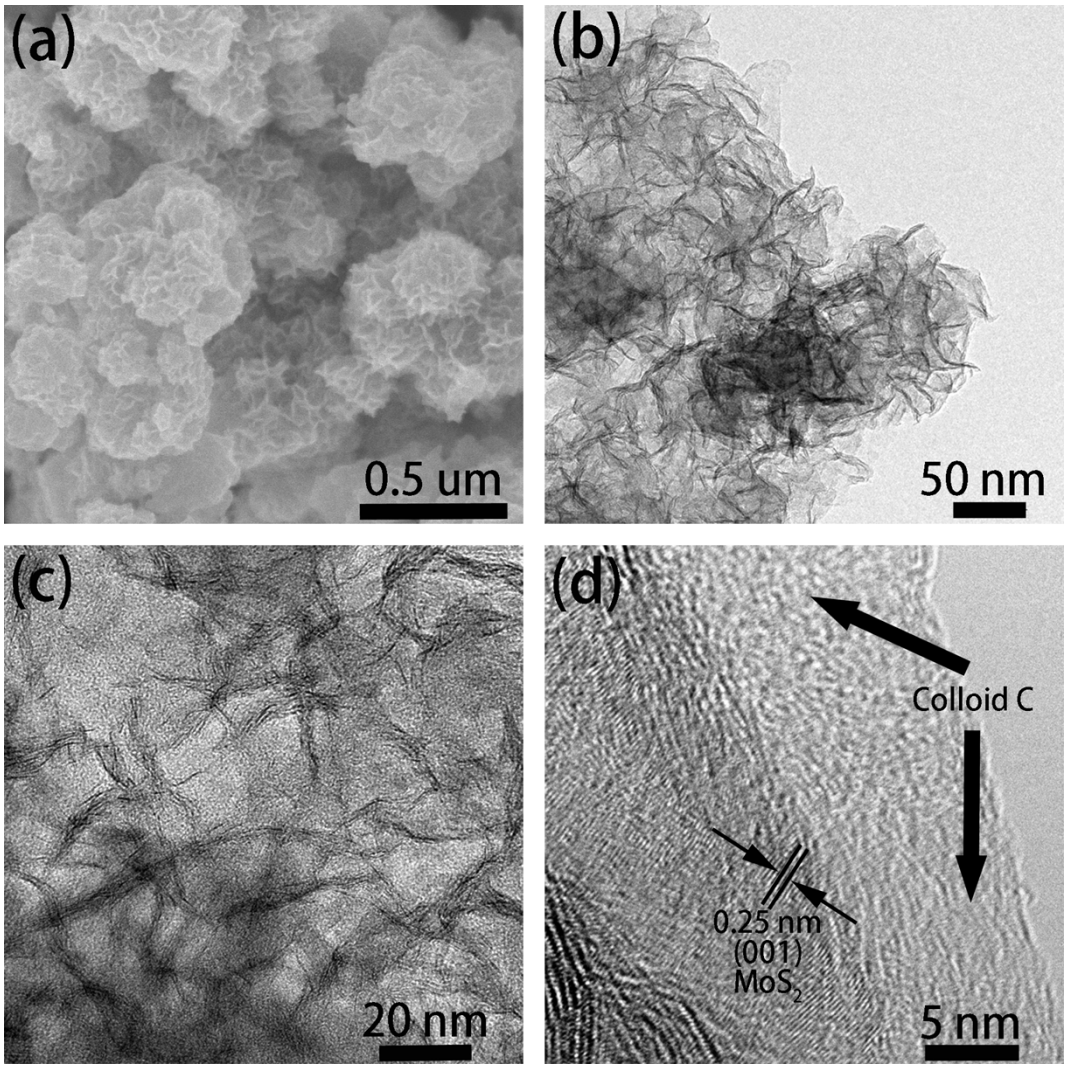

Fig. S3 (a) SEM image and (b-d) TEM images of hydrothermal products of the mixture of Na_2MoO_4-CN_2H_4S/glucose without F-TiO_2.

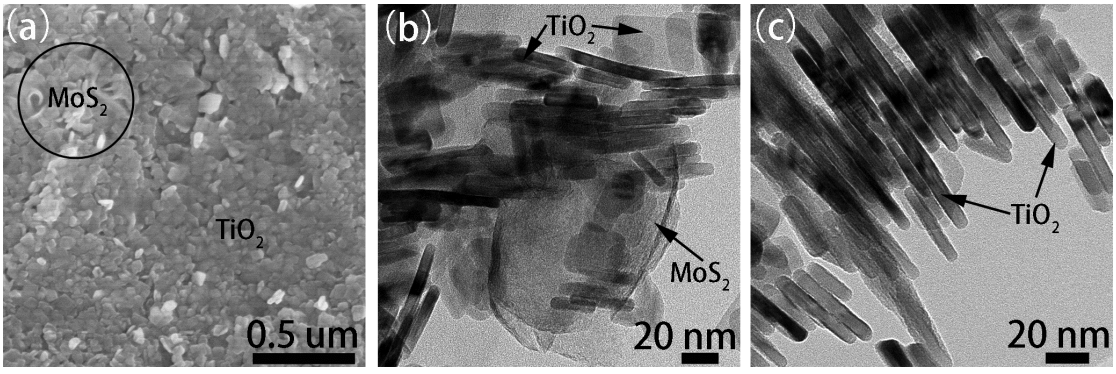

Fig. S4 (a) SEM image and (b, c) TEM images of hydrothermal products of the hybrid of Na_2MoO_4-CN_2H_4S/F-TiO_2 without glucose.

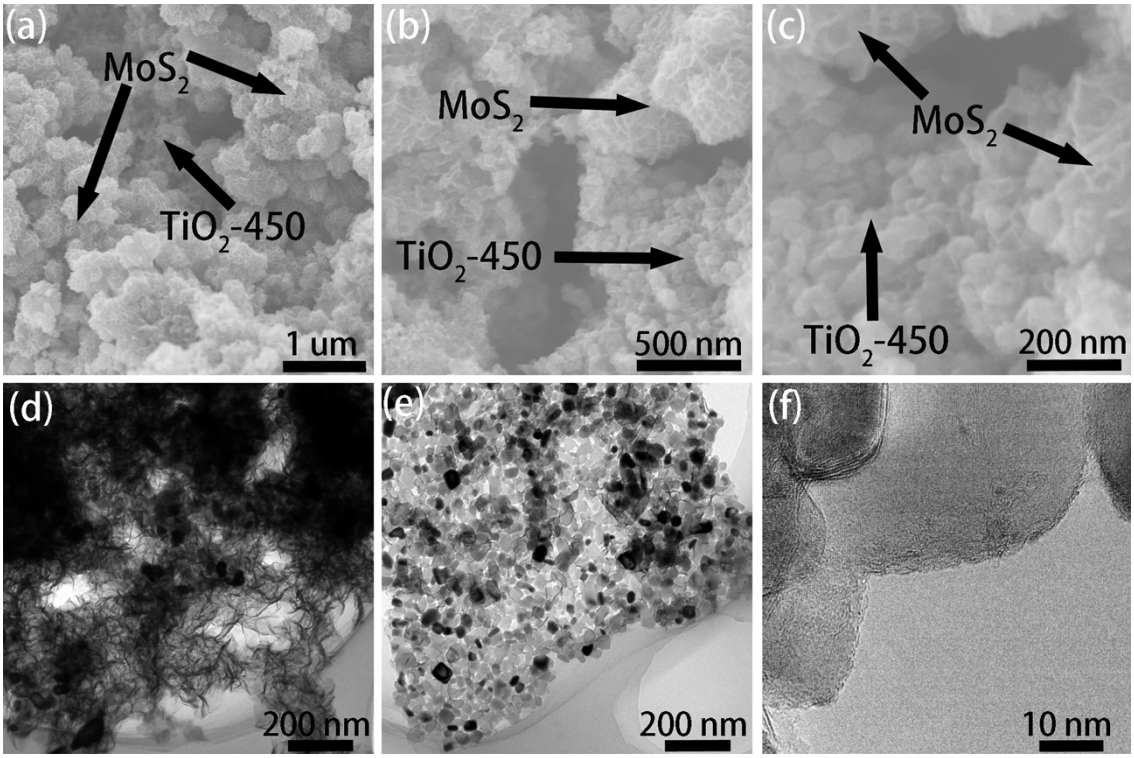

Fig. S5 (a-c) SEM images of MoS_2/TiO_2 composite before thermal-treated, (d-f) TEM images of MoS_2/TiO_2 composite after thermal-treated.

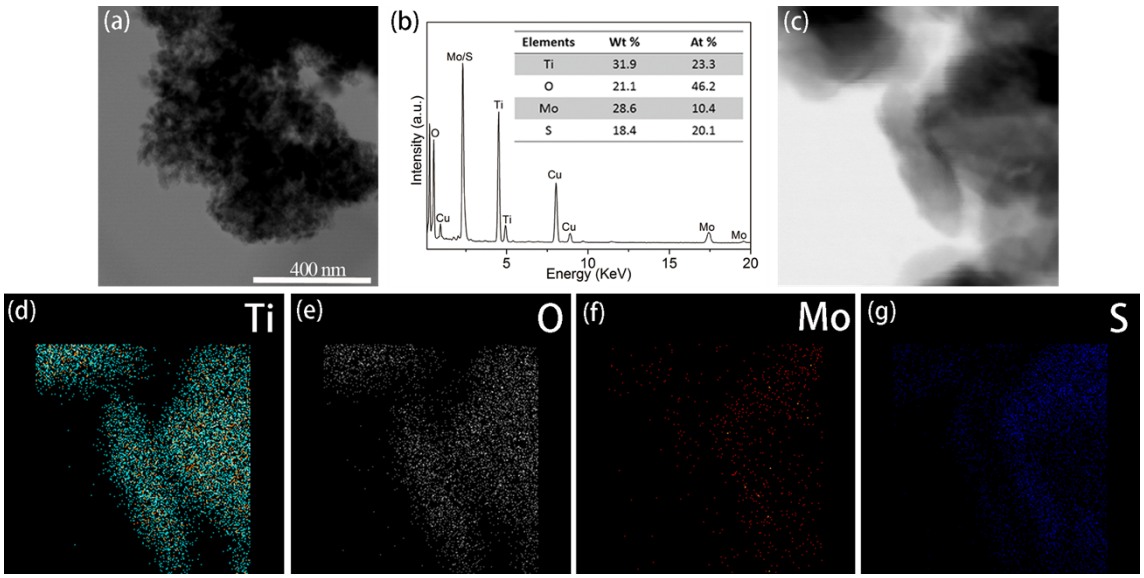

Fig. S6 (a) TEM image and (b) EDX spectra of a typical 3D FL-MoS_2@TiO_2. (c) STEM image of a detailed 3D FL-MoS_2@TiO_2, (d-g) corresponding EDX element mapping images of Ti, O, Mo, and S, respectively.

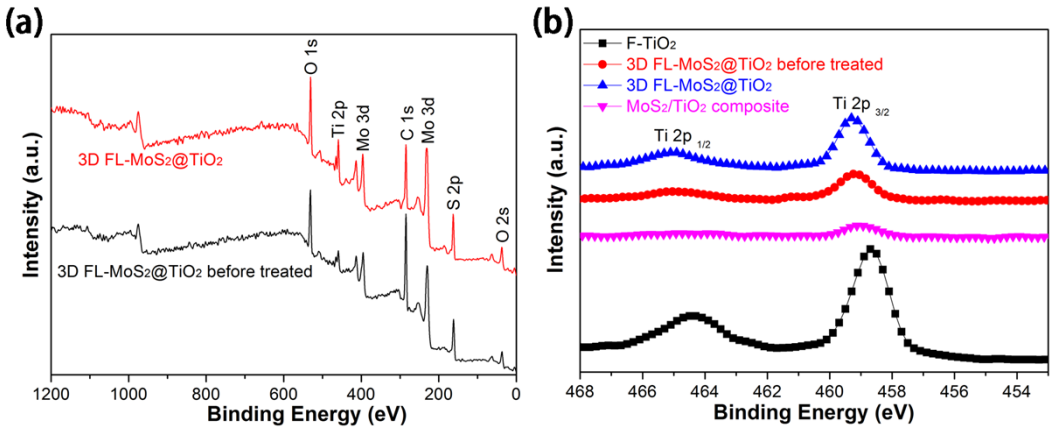

Fig. S7 (a) XPS survey spectra of the 3D FL-MoS_2@TiO_2 before and after calcination. (b) High-resolution XPS spectra of the Ti 2p region of F-TiO_2, MoS_2/TiO_2 composite, 3D FL-MoS_2@TiO_2 before and after calcination.

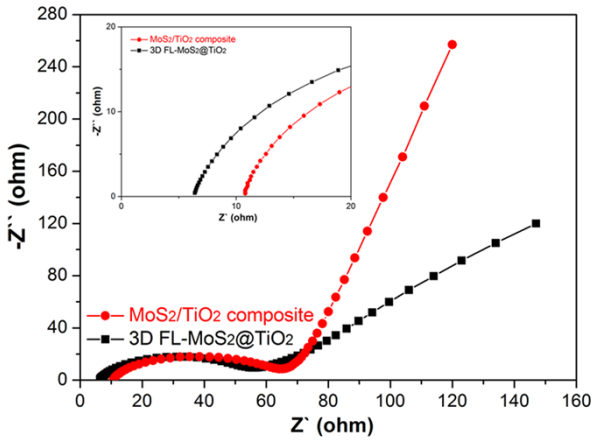

Fig. S8 Nyquist plots of 3D FL-MoS_2@TiO_2 and MoS_2/TiO_2 composite at the state of before cycling over the frequency range from 100 KHz to 100 mHz. The inset is the corresponding magnified high frequency region.

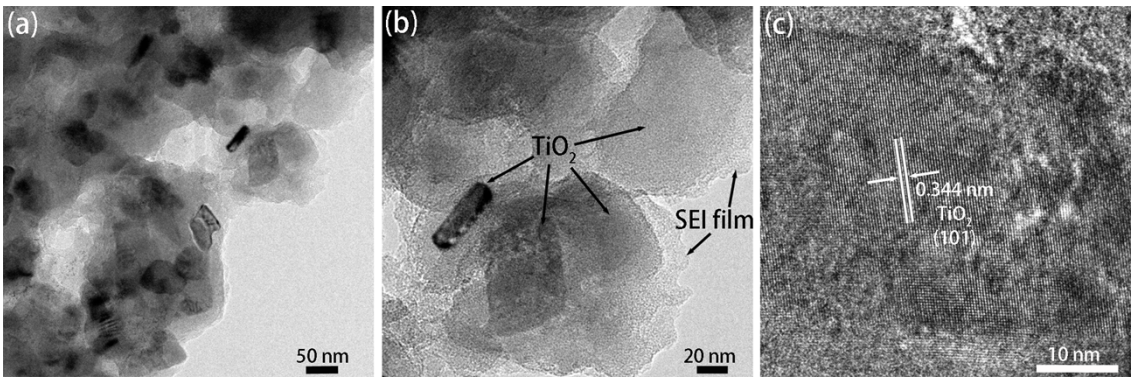

Fig. S9 (a-c) TEM images of the 3D FL-MoS_2@TiO_2 nanocomposite after the 150 electrochemical cycles for the rate cycle performance test in Fig. 6d.

Table S1 Detailed information of rate cycle performance of MoS_2, MoS_2/TiO_2 composite and 3D FL-$MoS_2@TiO_2$ electrodes corresponding to Fig. 6d.

Range of cycle	Charge/discharge rate (A/g)	Average charge capacity of MoS_2	Average charge capacity of MoS_2/TiO_2 composite	Average charge capacity of 3D FL-$MoS_2@TiO_2$
1-10	0.1	732.8	683.2	685.2
11-20	0.2	232.0	633.5	666.4
21-30	0.4	97.7	436.7	612.5
31-40	0.6	56.6	329.5	591.8
41-50	0.8	37.6	280.7	562.1
51-60	1.0	30.5	251.9	550.9
61-70	2.0	18.3	176.6	469.7
71-80	1.0	36.8	254.2	543.4
81	0.1	347.0	542.1	724.2
150	0.1	162.6	425.6	739.2

Table S2 Recently reported LIBs systems based on TiO_2 and MoS_2.

Marerials	Voltage range (V)	Charge capacity (mA h/g) at Current Density (mA/g) (capacity retention after cycle-index)	Rate capacity	Current Density(mA/g)
3D FL-MoS_2@TiO_2 [this work]	0.005-3.0	713.7 at 100 (95.9% after 100 cycles)	684.2 550.9 469.7 724.2	100 1000 2000 100
3D assembled MoS_2 [ref. 21]	0.01-3.0	839 at 100 (71.6% after 50 cycles) (discharge)	600 500 (discharge)	1000 5000
MoS_2 nanosheets [ref. 22]	0.01-3.0	750 at 50 (63% after 50 cycles) (discharge)	820 500 700 (discharge)	50 1000 100
MoS_2 microspheres [ref. 23]	0.01-3.0	585 at 100 (73% after 70 cycles)	726 353 700	200 1000 100
Ordered mesoporous MoS_2 [ref. 24]	0.01-3.0	645 at 50 (92% after 20 cycles)	640 220 580	50 1000 50
MoS_2 nanoflakes [ref. 25]	0.05-3.0	705.8 at 50 (70% after 40 cycles) (discharge)		
Anatase TiO_2 nanosheets [ref. 47]	1.0-3.0	136 at 850 (80.5% after 100 cycles)	192 95 169	170 3400 170
Anatase TiO_2 nanosheet [ref. 49]	1.0-3.0	120.2 at 850 (81.7% after 200 cycles)		
TiO_2 nanotube [ref. 58]	1.0-3.0	227 at 83.75 (100% after 100 cycles) (discharge)	267 176 260 (discharge)	33.5 3350 33.5
MoS_2 nanosheet@TiO_2 nanotube [ref. 42]	0.005-3.0	472 at 100 (68.1% after 100) (discharge)	713 461 611 (discharge)	100 1000 100
few-layered MoS_2@ TiO_2 nanobelt [ref. 43]	0.01-3.0	710 at 100 (91.5% after 100)	717 417 710	100 1000 100
MoS_2 nanosheet@TiO_2 nanowire [ref. 44]	0.01-3.0	544 at 100 (75.1% after 100) (discharge)	724 414 563 (discharge)	100 1000 100

Mesoporous MoS_2-TiO_2 nanofibers [ref. 45]	1.0-3.0	124 at 6000 (75.2% after 1000) (discharge)	188 177 120 187 (discharge)	1000 2000 40000 1000
TiO_2 microspheres embedded with MoS_2 nanosheets [ref. 46]	0.01-3.0	714 at 100 (86.2% after 200) (discharge)	962 450 805 (discharge)	100 1000 100
C@MoS_2 microspheres [ref. 26]	0.05-3.0	750 at 100 (~74% after 50) (discharge)	~780 500 750 (discharge)	100 1000 100
MoS_2/polyaniline nanowires [ref. 27]	0.01-3.0	952.6 at 100 (89.6% after 50)	1006.4 320 900	200 1000 200
MoS_x/CNT Nanocomposites [ref. 29]	0.01-3.0		1119 358 197 1087 (discharge)	50 1000 2000 50
CNT@MoS_2 [ref. 30]	0.01-3.0	698 at 100 (48.7% after 60) (discharge)	653 389 (discharge)	200 1000
MoS_2–MWCNT hybrids [ref. 31]	0.01-3.0	1090 at 100 (89.8% after 30)	~870 ~550 ~1000	200 500 100